Available online at www.sciencedirect.com
SCIENCE DIRECT®
Journal of Magnetic Resonance 170 (2004) 220–227
JMR Journal of Magnetic Resonance
www.elsevier.com/locate/jmr

# Determination of $T_1$-spin–lattice relaxation time in a two-level system by continuous wave multiquantum electron paramagnetic resonance spectroscopy in a presence of tetrachromatic microwave irradiation

Małgorzata Dutka*, Ryszard J. Gurbiel, Jerzy Kozioł, Wojciech Froncisz

*Department of Biophysics, Faculty of Biotechnology, Jagiellonian University, Gronostajowa 7, 30-387 Kraków, Poland*

Received 11 February 2004; revised 30 June 2004
Available online 29 July 2004

**Abstract**

Applicability of continuous wave multiquantum EPR methods to study relaxation times at X-band is examined. Multiquantum transitions excited in a two-level system by tetrachromatic irradiation are used for these studies. The Bloch equation model is applied to simulate lineshapes of the three quantum transitions as a function of frequency difference between exciting fields. The dependence of multiquantum transition signals on relaxation times and microwave amplitude is shown. On this basis a method of deducing relaxation times from these signals is formulated. The case of a homogeneously and inhomogeneously broadened resonance line is considered. Two experimental methods are used to verify the proposed hypothesis: the X-band continuous wave multiquantum EPR with four frequencies microwave field and saturation recovery EPR. The values of $T_1$ obtained from CW MQ EPR and SR EPR are compared.


*Keywords:* Continuous wave multiquantum electron paramagnetic resonance; Multiphoton transitions; Longitudinal relaxation time; Nitroxide spin labels; Inhomogeneous broadening

## 1. Introduction

Electron paramagnetic resonance (EPR) techniques are widely used as a spectroscopic tool for obtaining information about molecular mobility. Within that area of research experiments aimed at the study of relaxation phenomena driving the magnetization to the thermal equilibrium are developed. Advantages of such an approach are pronounced if only the problem of connection between observed electron spin–lattice relaxation rates and molecular dynamics is solved. Applications of EPR spectroscopy grow extensively in the field of structural and dynamical investigations of biological systems [1]. Specially the development of site-directed spin labeling [2] has created the need for methods of retrieving information from EPR signals.

The consciousness of difficulties in finding direct dependence upon the rotational correlation time, and elucidating the underlying mechanism of molecular dynamics has accompanied the development of the $T_1$—sensitive EPR techniques [3,4]. Recently a model explaining electron relaxation mechanism of $T_1$ of nitroxides in liquids for viscosities covering eight orders of magnitude has been proposed [5]. The range of motional effects investigated using EPR methods has been extended due to direct dependence of $T_1$ upon the rotational correlation time, observed when the motion of the paramagnetic species slows down [6–8]. The exchange and dipolar interactions are other mechanisms that can mod-

* Corresponding author. Fax: +48-12-664-6902.
*E-mail address:* mdutka@mol.uj.edu.pl (M. Dutka).

1090-7807/$ - see front matter 
doi:10.1016/j.jmr.2004.07.002

ify the electron spin–lattice relaxation rates. Measurements of $T_1$ found applications in oximetry [9], studies of spin label accessibility to other paramagnetic species [10] or measurements of inter-spin distances [11].

To determine the value of electron spin–lattice relaxation the continuous wave and pulsed EPR techniques have been used [12–15]. Using time domain EPR methods—saturation recovery or pulsed ELDOR (electron–electron double resonance) [3]—one can directly estimate $T_1$. The multicomponent nature of the observed signals can cause serious problems in analysis of the data. Separation of the existing decay rates is possible by performing SR and ELDOR experiments, and then pooling acquired data [16]. After such a 'signal decomposition'' procedure one can find that the true electronic spin lattice relaxation time, $T_{1e}$, determines the decay of one component, whereas other components contained in the experimental signal result from the nuclear relaxation or other mechanisms of spectral diffusion. The detailed study of an electron spin lattice relaxation reveals its multicomponent character as an inherent feature [17]. At a given temperature an energy transfer form the spin system to the bath is realized via different mechanisms (e.g., the Raman process, spin–orbit coupling, thermally activated motions). Their simultaneous contribution brings about many-exponential time-dependence of the observed signal [18]. The single exponential saturation recovery signal occurs only when a single process dominates relaxation.

Determination of the relaxation times from CW experiments is indirect and complicated by the inhomogeneous spectral broadening. Using the conventional, progressive saturation EPR [8,13] methods, the product $(T_1T_2)^{-1}$ is obtained and an additional effort has to be made for an estimation of the correct $T_2$ value, especially in case of complicated, non-Lorentzian EPR lineshapes. There have been recently developed procedures of extraction of $T_1$ from progressive saturation EPR curves for spin labels spectra [8,13]. In another approach analysis of the first harmonic out-of-phase absorption EPR signal allowed for determining $T_1$-enhancements [19].

Within continuous wave EPR methods only signals generated by nonlinear effects demonstrate enhanced sensitivity to spin–lattice relaxation. A nonlinear response of a spin system to an applied external modulation (static magnetic field modulation, or microwave field modulation) is crucial for retrieving relaxation information from the continuous wave EPR experiment. Complete theoretical description of that physical situation is complicated because: (1) an external radiation field is not monochromatic, (2) coupling of the spin system to the ''thermal bath'' must be included explicitly, and (3) in many cases multi-level instead of the simplest two-level spin system must be considered. The real, unavoidable hindrance appears in calculations (either analytical or numerical) due to coupling between harmonics of the signal, in the presence of the relaxation mechanisms. Different formalisms can be applied to describe interaction between a spin ensemble and an external polychromatic field: second quantization formalism [20], density matrix equations [21], and modified Bloch equations [22]. In many cases introduction of relaxation via phenomenological constants $T_1$ and $T_2$ is sufficient but sometimes a full stochastic description of the relaxation mechanisms is required. Recently developed general theory of the nonlinear response of a multi-level spin system subjected to external fields [23] has brought some conclusions adequate to X-band EPR domain. It has been shown that a signal observed as a nonlinear response of a spin system subjected to weak multiple irradiation explicitly depends on $T_1$.

The case of nitroxide spin labels must be considered as a system with spin S = 1/2 coupled to a nucleus with I = 1. At X-band we observe that: (1) hyperfine splitting constant $\omega_I$ is much less than Larmor frequency $\omega_0$ and (2) occurs ''time scale separation'' between the longitudinal relaxation and microscopic correlation time $\tau_c$ of interactions relaxing the magnetization. Under these assumptions the single exponential decay of a longitudinal magnetization can be expected in that system [24]. The time constant, $T_1$, is ascribed to true, intrinsic electronic relaxation time. The most interesting aspect of the experiment with bichromatic microwave irradiation (at $\omega_1$ and $\omega_2$) is a measurement of the EPR signal amplitude as a function of the frequency difference $\omega_1 - \omega_2$. The theory [23] supports the conclusion that in this case true electronic $T_1$ can be obtained, contrary to progressive saturation or saturation transfer methods yielding the value of $T_1$ effective. The experimental verification of this statement has been carried out by Cianflone et al. [14].

Multiquantum EPR spectroscopy is thoroughly devoted to observation of essentially nonlinear, intermodulation signals, and retrieving from them information about an investigated system. Methods belonging to that branch use polychromatic microwave field to irradiate the investigated system, whereas no static magnetic field modulation is necessary for detection. An outcoming overall EPR signal is composed of many intermodulation sidebands due to multiquantum transitions taking place in the irradiated spin system. Its frequency spectrum contains not only introduced components but additional ones, resulting from mixing of the incident fields by the spin system A sideband ascribed to a chosen *n-quantum* process is then *selectively* detected by setting the proper frequency of the reference field. In particular, double frequency [25,26] and four frequency [27] microwave irradiation (at X-band) was used to excite multiple quantum transition. The properties of that ''quantum mixer,'' especially relaxation rates, determine the amplitude and shape of the recorded spectrum. It is known that at low incident power the amplitudes of 3 and 5 quantum processes are proportional to $T_1$ [28]. Analysis

of the multiquantum signal amplitude as a function of the frequency difference between the incident microwave fields gives information about the relaxation times. It has been demonstrated that longitudinally detected EPR signal (LODESR), observed in the system irradiated by a bichromatic microwave field, has a width equal to $(T_1)^{-1}$ and is not affected by the inhomogeneity [14]. The signals detected in a transversal plane also show sensitivity to the longitudinal relaxation time [15,28]. They are especially convenient to monitor relative changes in $T_1$ [29].

The aim of the present work is to develop and examine an integrated method of deducing relaxation times values from multiquantum EPR transitions. We examine the $T_1$-dependence of the three quantum EPR signals, observed experimentally in a two-level system excited with a four frequency microwave irradiation.

## 2. Theory

### 2.1. Intermodulation observed upon tetrachromatic irradiation of the spin system

Generation of multiquantum (MQ) transitions under EPR conditions can take place in a spin system irradiated with polychromatic electromagnetic field. Application of continuous polychromatic irradiation (at X-band) has brought unique effects within EPR spectroscopy [25,30], due to the advantageous relation between paramagnetic relaxation rates and frequency difference of the exciting fields. An observed signal is composed of many intermodulation components occuring at different frequencies, which arise from the multiquantum transitions [28]. A classical model of resonance, based on the modified Bloch equations, is of practical value to describe these nonlinear effects [31]. In a real experiment a chosen multiquantum signal can be detected selectively, as a function of the swept magnetic field and a pure absorption or dispersion line can be recorded. In case of negligible saturation the amplitude of the three quantum transition (3QT) is proportional to $T_1$ [28,29]. In general the half-width of the curve representing absolute amplitudes of the 3QT CW EPR spectra vs frequency difference of the microwave fields is affected by the relaxation rates of the sample as well as by the saturation factor [31].

In experiments reported here continuous wave, four-frequency microwave irradiation is used to excite multiphoton transition in a two-level system [27]. The four components of the incident field (with frequency $\omega_i$ and amplitude $B_i$) fulfill the following conditions:

$$\omega_{1,4} = \omega_C \pm (\Omega + \delta); \quad \omega_{2,3} = \omega_C \pm \Omega; \tag{1}$$

$$\delta/2 < \Omega < \Delta\omega_0, \tag{2}$$

where $\omega_i (i = 1,\ldots,4)$—the frequencies of the irradiating fields; $\omega_C$—the microwave carrier frequency; and $\Delta\omega_0$—halfwidth of the resonance line.

The components of the tetrachromatic microwave field are placed symmetrically with respect to the carrier frequency and create two pairs: ($\omega_1$, $\omega_2$) and ($\omega_3$, $\omega_4$). Separation between pairs (which is equal to $2\Omega$) is greater than the difference within the pair ($\delta$).

The chosen frequencies are close to the resonance: $\Omega < 10^{-4}\omega_0$ and $\Omega, \delta < T_{1,2}^{-1}$ ($\omega_0$ denotes the resonance frequency). All four fields have equal amplitudes: $B_i = B_1$. The response of a two-level system to such an irradiation has been explained on the ground of Many Mode Floquet Theory [27].

The signal emitted from the system contains the intermodulation sidebands at frequencies:

$$\omega_{\pm k \pm l} = \omega_C \pm k\Omega \pm l\delta (k > 0, l \geqslant 0). \tag{3}$$

If $k = 1$ we call the signals as "close" sidebands; all others we call "far." A given component results from a multiphoton process that engages the photons from the four fields [27]. The analytical formulas describing these signals, taking into account relaxation and nonnegligible saturation, cannot be found on the ground of quantum mechanics. To simulate a spin system response to tetrachromatic excitation we have employed previously developed [31] computational procedure of solving modified Bloch equations (BE) with two-frequency irradiation. An introduction of the second pair of exciting fields required only a trivial modification of the matrix containing coefficients of the BE. The applied Gear's algorithm [32] enables very high efficiency in solving that set of linear differential equations with periodic coefficients, even when the values of $T_1$ and $T_2$ make them "stiff."

### 2.2. Determination of $T_1$ from multiquantum signals

The model based on the classical Bloch equations, where the four frequency alternating field is incorporated, has appeared to be a very effective tool in a qualitative and semi-quantitative analysis of a considered phenomenon. The intermodulation sidebands created in a two-level system excited with four frequency microwave fields exhibit more complicated frequency pattern than in case of bichromatic perturbation. Fig. 1 shows the magnitude frequency spectrum of the overall signal, composed of many sidebands. The frequency pattern of the incident exciting field is shown on the lower diagram. We confine our attention to signals appearing at frequencies:

$$\omega_0 \pm (\Omega - \delta), \omega_0 \pm (\Omega + 2\delta) \tag{4}$$

and

$$\omega_0 \pm (3\Omega + \delta), \omega_0 \pm (3\Omega + 2\delta). \tag{5}$$

All of them originate from three photon processes [27]. The sidebands surrounding incident fields (Eq. (4)) are, as defined above, "close" three quantum transi-

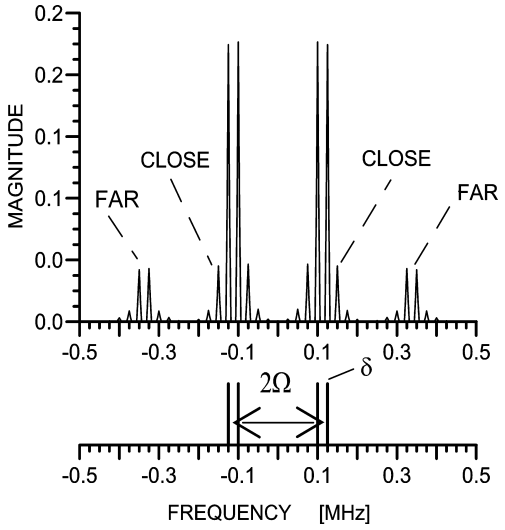


Fig. 1. The frequency spectrum of the simulated signal excited in the two level system subjected to the tetrachromatic irradiation. Parameters for simulations are: $T_1 = 1\,\mu s$, $T_2 = 0.4\,\mu s$, $B_1 = 0.04\,G$, $\Omega = 100\,kHz$, and $\delta = 25\,kHz$. The lower diagram shows the pattern of the incident field. The carrier frequency of the microwave field is equal to the resonance frequency. "Close" 3QT transitions appear at 75 and 150 kHz; "far" 3QT are at 325 and 350 kHz.

tions (3QT) and this part of the frequency spectrum (Fig. 1) resembles the picture known from the two-frequency CW MQ experiment [25]. The distant group of sidebands appears in the four-frequency experiment and represents "far" 3QT (Eq. (5)). The previously reported experiments [27] demonstrated the same saturation characteristics and sensitivity to changes of $T_1$ for "close" and "far" signals ascribed to 3QT.

The purpose of the performed simulations is to investigate the dependence of the selected sideband amplitude on $T_1$, $T_2$, $\delta$, $\Omega$, and $B_1$. The resonance line for a particular sideband is obtained sweeping the static magnetic field, whereas $\Omega$ and $\delta$ are kept constant. Simulated absorption and dispersion spectra for both "close" and "far" sidebands exhibit inherent phase change when $\Omega$ increases, which reproduces features observed experimentally. Studying the dependence of "close" and "far" sidebands amplitude (at the center of the line: $\omega_C = \omega_0$) on the frequency difference $\Omega$ seems to be the most promising for practical applications. A lineshape of a multiquantum signal is affected not only by that "inherent phase changes" but also by an undefined change of the microwave phase. In order to preserve the complete information about the spin system response to the polychromatic excitation, *in phase* and *out-of-phase* signals must be recorded. As $\Omega$ increases to the values comparable to $T_1^{-1}$, the out-of-phase part of the signal becomes significant. Unambiguous analysis of the signal dependence on increasing $\Omega$ is possible if its absolute magnitude, independent of the phase, is taken. That difficulty has already appeared in experiments with bichromatic excitation [31], where also phase sensitive signal detection is applied.

Fig. 2 shows simulated $\Omega$-dependencies of the absolute amplitude for "close" and "far" intermodulation sidebands, related to three quantum transitions. The influence of the $\delta$ value on the shape of the profile $|S_{3QT}(\Omega, B_1^2)|_{\delta=const}$ is negligible provided that $\delta \ll \Omega$ and $\delta \ll (2\pi\ T_1^{-1})$ (in practice $\delta = 5\,kHz$ is sufficient to fulfill both conditions). In general the half-width, $\Delta_{1/2}$, of the "frequency sweep" characteristics is always greater for "close" sidebands and also depends on the incident microwave power. The parameter $\Delta_{1/2}$ is a function of $T_1$, $T_2$, and $B_1$.

The first observation resulting from the simulation is that $\Delta_{1/2}$ is determined mainly by $T_2^{-1}$ for "close" sidebands and $T_1^{-1}$ for "far" sidebands, but does not reflect directly relaxation rates. The saturation characteristics of the "close" and "far" 3QT are identical, as it has been shown previously [27]. How to explain the different $\Omega$-dependent characteristics? The physics of intermodulation sidebands generation enforces the following condition: $(\omega_i - \omega_k) < T_1^{-1}$, where $\omega_{i,k}$ denote the frequencies of the polychromatic irradiation applied to the spin system. In case of a tetrachromatic microwave field we have $|\omega_2 - \omega_3| = 2\Omega$ and $|\omega_1 - \omega_2| = |\omega_3 - \omega_4| = \delta$. The close sidebands occur at frequencies $\pm(\Omega \pm l\delta)$ [27] (the reference frame is rotating at the resonance frequency) and result from mixing between closely spaced components within pairs $\omega_1$ and $\omega_2$ or $\omega_3$ and $\omega_4$. The value of $\delta$ is chosen to be small (a few kHz) and kept constant, so condition: $\delta < T_1^{-1}$ is always fulfilled. As $\Omega$ increases up to the homogeneous packet linewidth ($\Omega \approx T_2^{-1}$), the resonance condition breaks down and practically the system does not interact with

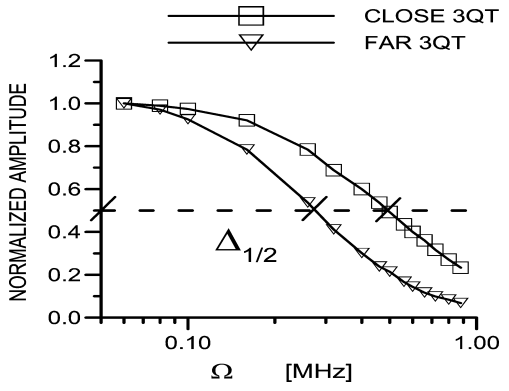


Fig. 2. The simulated traces of $|S_{3QT}(\Omega)|$for $T_1 = 0.35$ and $T_2 = 0.20\,\mu s$. For all simulations parameter $\delta$ was kept constant (5 kHz). A single point represents a calculated amplitude of a multiquantum signal at a given value of $\Omega$. Values obtained for a series of $\Omega$ create a profile drawn as a solid line. Normalized profiles for three quantum transitions "close" and "far" are shown. Amplitude of exciting fields is equivalent to microwave power 0.016 mW. From such a display the parameter $\Delta_{1/2}$ is read (for "close" and "far" signals).

the irradiation. Contrary to this, the appearance of "far" intermodulation sidebands involves mixing distant components of the field (e.g., 1, 2, and 3 or 1, 3, and 4, etc.) The amplitude of 3QT "far" is significant only if $\Omega < T_1^{-1}$ holds true.

The half-width $\Delta_{1/2}$ of the $\Omega$-dependent characteristics of 3QT transitions is affected by the saturation factor, not known a priori. For that reason $\Delta_{1/2}$ cannot be related directly to the relaxation rates. An example of a dependence of $\Delta_{1/2}$ on $B_1^2$ (obtained from the simulations) is shown in Fig. 3. To eliminate the contribution from microwave power we extrapolate that function to the value $B_1^2 = 0$ and define the parameter:

$$\Delta_0 = \lim_{B_1^2 \to 0} \Delta_{1/2}(T_1, T_2, B_1^2). \quad (6)$$

The systematic simulations have been carried out to cover the extensive space of parameters $T_1$ and $T_2$, taking into account also their ratio $T_1/T_2$. We have compared the parameters $\Delta_0^{\mathrm{CLOSE}}$ and $\Delta_0^{\mathrm{FAR}}$ extracted after computations with relaxation rates introduced initially. Figs. 4A and B show, respectively, the values of the products: $2\pi\Delta_0^{\mathrm{FAR}} \cdot T_1$ and $2\pi\Delta_0^{\mathrm{CLOSE}} \cdot T_2$, which are constant over a wide range of $T_1/T_2$. Table 1 contains proposed formulas which relate parameters $\Delta_0^{\mathrm{CLOSE}}$, $\Delta_0^{\mathrm{FAR}}$, and relaxation times. The presented procedure of estimating $T_1$ from $\Delta_0^{\mathrm{FAR}}$ gives better accuracy for greater ratio $T_1/T_2$. If relaxation times become comparable ($T_1/T_2 < 2$), the decay of an amplitude of 3QT "FAR" as $\Omega$ increases, results from both longitudinal and transversal mechanisms. A proposed formula $T_1 = \frac{1}{2} \cdot \frac{1}{2\pi\Delta_0^{\mathrm{FAR}}}$ working in this region gives accuracy up to 30%. Simulations showed that the ratio $\gamma = \Delta_0^{\mathrm{CLOSE}}/\Delta_0^{\mathrm{FAR}}$ allows for a priori discrimination between cases $T_1 \gg T_2$ and $T_1 \cong T_2$. If $T_1 \gg T_2$, 3QT "far" signals decay is dominated first by the longitudinal relaxation. Its value can be obtained from the equation $T_1 = \frac{1}{2\pi\Delta_0^{\mathrm{FAR}}}$, with an error less than 10%. The bigger error is for $T_1 \cong 3T_2$ when the ambiguity of choosing the proper formula is the highest. Basing on the results shown in Fig. 4B the following formula for extracting $T_2$ can be proposed: $T_2 = \frac{1}{2} \cdot \frac{1}{2\pi\Delta_0^{\mathrm{CLOSE}}}$. It gives correct values of $T_2$ (within 10% error) over whole range ofthe ratio $T_1/T_2$, but only for homogeneous system.

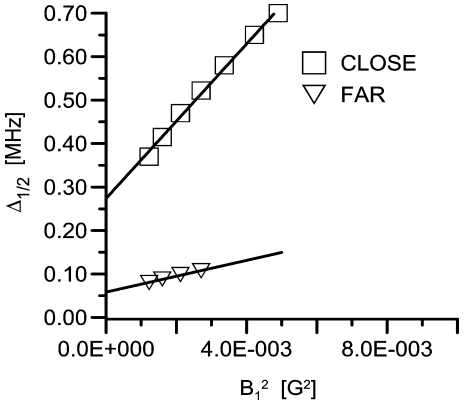


Fig. 3. The dependence of parameter $\Delta_{1/2}^{\mathrm{FAR}}$ and $\Delta_{1/2}^{\mathrm{CLOSE}}$ on $B_1^2$. Numerical simulations were carried out for $T_1 = 3\,\mu s$ and $T_2 = 0.4\,\mu s$. The extrapolation to $B_1^2 = 0$ gives the value of $\Delta_0$ (the linear function is fitted to the points representing the values of $\Delta_{1/2}^{\mathrm{FAR}}$ and $\Delta_{1/2}^{\mathrm{CLOSE}}$ calculated for consecutive $B_1$).

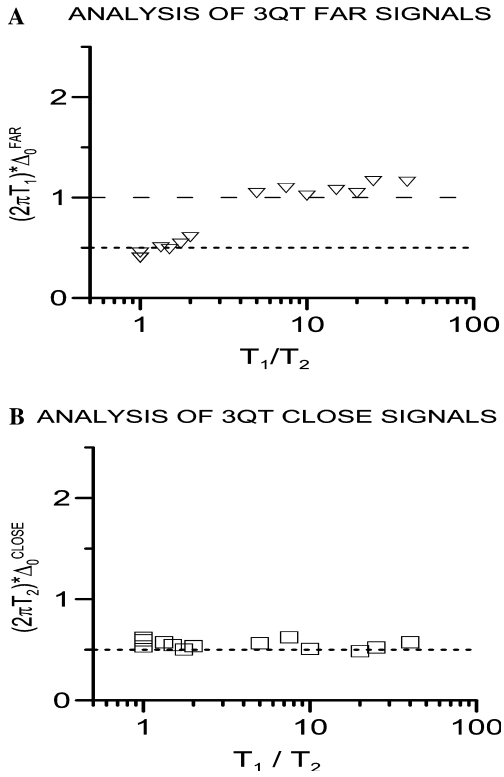


Fig. 4. (A) The dependence of the product $2\pi\Delta_0^{\mathrm{FAR}} \cdot T_1$ on the ratio $T_1/T_2$. The parameter $\Delta_0^{\mathrm{FAR}}$ has been extracted from the simulated traces $|S_{3QT}(\Omega,B_1)|$of 3QT "far" signals (see Eq. (6)) for several sets of initial parameters $(T_1,T_2)$. The product: $2\pi\Delta_0^{\mathrm{FAR}} \cdot T_1$ (its value marked by a symbol) is approximately equal to 1 for $T_1 \gg T_2$, and equal to 0.5 for $T_1 \cong T_2$ (values $2\pi\Delta_0^{\mathrm{FAR}} \cdot T_1 = 12\pi\Delta_0^{\mathrm{FAR}} \cdot T_1 = 0.5$ are marked as dotted lines). (B) The dependence of the product $2\pi\Delta_0^{\mathrm{CLOSE}} \cdot T_2$ on the ratio of $T_1/T_2$. The parameter $\Delta_0^{\mathrm{CLOSE}}$ has been extracted from the simulated traces $|S_{3QT}(\Omega,B_1)|$of 3QT "close" signals (see Eq. (6)) for several sets of initial parameters $(T_1,T_2)$. The product: $2\pi\Delta_0^{\mathrm{CLOSE}} \cdot T_2$ (represented by a symbol) is constant and approximately equal to 0.5 over wide range of parameters $T_1$ and $T_2$. ($y = 2\pi\Delta_0^{\mathrm{CLOSE}} \cdot T_2$ is marked as a dotted line).

Table 1
Formulas proposed to relate the parameters $\Delta_0 = \Delta_{1/2}(B_1^2 \to 0)$ with relaxation times

| $\Delta_0$ | $T_1 \approx T_2$ | $T_1 \gg T_2$ |
|---|---|---|
| $\Delta_0^{\mathrm{FAR}}$ | $\frac{1}{4\pi T_1}$ | $\frac{1}{2\pi T_1}$ |
| $\Delta_0^{\mathrm{CLOSE}}$ | $\frac{1}{4\pi T_2}$ | $\frac{1}{4\pi T_2}$ |

$\Delta_0^{\mathrm{FAR}}$ denotes parameter $\Delta_0$—approximated half-width of the profile $|S_{3QT}(\Omega)|$in the limit $B_1^2 \to 0$ obtained for 3QT "far" signals; and similarly $\Delta_0^{\mathrm{CLOSE}}$—obtained for 3QT "close" signals.

To make model more realistic we include the effect of inhomogeneous broadening into our simulations. The profiles $| S_{3QT}(\Omega, B_1^2)|_{\delta=\mathrm{const}}$ were computed assuming dif-

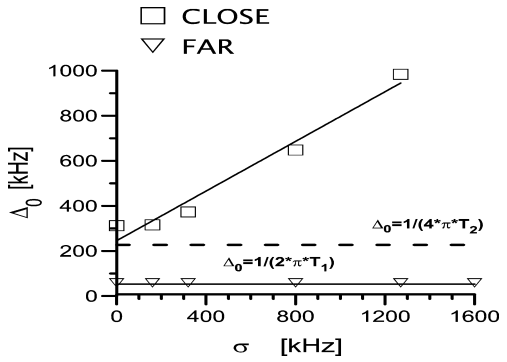


Fig. 5. The dependence of the parameter $\Delta_0$ on the width of an inhomogeneous packet. The parameters $\Delta_0^{\mathrm{CLOSE}}$ and $\Delta_0^{\mathrm{FAR}}$ (represented by squares and triangles) are computed for the system with relaxation times: $T_1 = 3\,\mu s$ and $T_2$=0.35 μs and increasing width of an inhomogeneous packet, $\sigma$. The horizontal lines mark values: $\Delta_0 = 1/4\pi T_2$ and $\Delta_0 = 1/2\pi T_1$. $\Delta_0^{\mathrm{FAR}}$ is not influenced by inhomogeneity of the spin system. $\Delta_0^{\mathrm{CLOSE}}$ is affected by the $\sigma$ (points $\Delta_0^{\mathrm{CLOSE}}$ and a line $\Delta_0 = \sigma$ are shown).

ferent values of the inhomogeneous packet width $\sigma$. The parameters $\Delta_0^{\mathrm{FAR}}$ and $\Delta_0^{\mathrm{CLOSE}}$ were extracted from them. The first conclusion from simulation is that formula $\Delta_0^{\mathrm{CLOSE}} \cong 1/4\pi T_2$ fails in case of inhomogeneous system and is a function of $\sigma$, which follows intuition. Much more interesting result is that parameter $\Delta_0^{\mathrm{FAR}}$ still reasonably well reproduces the longitudinal relaxation rate and does not depend on $\sigma$ (Fig. 5). The conclusion is that in case of long longitudinal relaxation rates ($T_1 \gg T_2$) the parameter $\Delta_0^{\mathrm{FAR}}$ directly reflects $T_1$, regardless of inhomogeneity of the system.

## 3. Experimental results

### 3.1. Experimental procedure

Experimental studies were carried out on a multipurpose, home assembled EPR X-band spectrometer, capable of performing standard CW EPR, pulsed saturation recovery EPR and multiquantum EPR measurements [27]. Detailed description of a microwave bridge can be found in [27]. The samples were placed in a 1 mm loop-gap resonator [33]. $Q$ (loaded) for the empty resonator was equal to 360 (frequency 9.3446 GHz). For comparison $Q$ measured for the resonator with TPX water-filled capillary was 221. In the experiments reported here the critical coupling of the resonator was assured.

Three quantum EPR signals (in absorption and dispersion mode) were recorded in two channels (in phase and 90° out of phase with respect to the low frequency reference) for fixed value of frequency separation $\delta$ and for several values of $\Omega$. The values of $\Omega$ varied in the range from tens of kHz up to 5 MHz; $\delta$ was not greater than 10 kHz. The measurements were carried out for several values of microwave power irradiating the samples. The equal amplitudes of all four components of a microwave field were assured. On the same samples the measurements of saturation recovery EPR were carried out [34]. The experimental decay curves were obtained using optimal pump and observing pulses.

### 3.2. Samples

The liquid samples of paramagnetic species: an aqueous solution of the spin label TEMPONE; aqueous solution of TEMPOL in 80% glycerol and aqueous solution of Fremy's salt (PADS) were used. The solution of PADS (Sigma Chemical) was freshly prepared from solid and buffered with 50 mM $K_2CO_3$ in order to reduce the rate of decomposition. Sample concentrations were 1 mM. The liquid samples were placed in a TPX capillary and equilibrated with flowing nitrogen during the measurements. Temperature was set at +21 °C. Additionally measurements of 1 mM TEMPOL in glycerol–water mixture were carried out at +10 °C.

### 3.3. Results and discussion

Experiments were carried out using two methods: CW MQ EPR method with four-frequency microwave field and long pulse saturation recovery EPR. The traces $|S_{3\mathrm{QT}}(\Omega, B_1^2)|_{\delta=\mathrm{const}}$ were measured for each type of sample. As an example the series of such profiles for several values of $B_1^2$ is shown in Fig. 6. Following the procedure described in Section 2.2 the parameter $\Delta_0^{\mathrm{FAR}}$ was determined, then the value of $T_1$ was calculated from it. Independently the measurements of saturation recovery EPR signals on those samples gave directly the values of $T_1$. These results are summarized in Table 2, where relaxa-

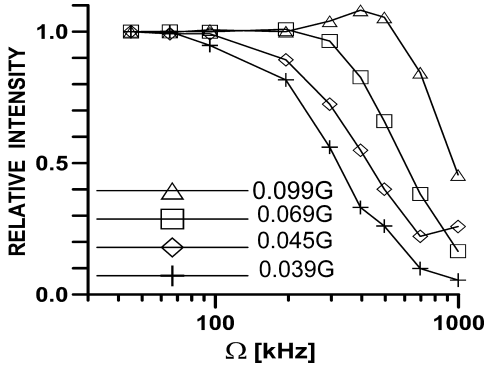


Fig. 6. The measured dependence of 3QT "far" magnitude on the frequency difference $\Omega$. The sample was 1 mM PADS in the nitrogen atmosphere. The traces were recorded for decreasing level of microwave power. The microwave amplitude $B_1$ is calculated from the relation: $B_1 = \Lambda\sqrt{P}$; $P$—microwave power in Watts, $\Lambda$—conversion efficiency of the loop-gap resonator, here is equal to 5. The value of $\delta$ was equal to 5 kHz and kept constant.

Table 2
Spin–lattice relaxation time $T_1$ obtained from CW multiquantum EPR method and saturation recovery EPR

| Sample | MQ (μs) | SR (μs) | Case |
|---|---|---|---|
| PADS[a] | 0.48 ± 0.10 | 0.38 ± 0.02 | $T_1 \cong T_2$ |
| TEMPONE[b] | 0.69 ± 0.10 | 0.57 ± 0.03 | $T_1 > T_2$ |
| TEMPOL in glyc. +21 °C | 2.2 ± 0.30 | 2.3 ± 0.12 | $T_1 \gg T_2$ |
| TEMPOL in glyc. +10 °C | 3.45 ± 0.50 | 3.3 ± 0.16 | $T_1 \gg T_2$ |

Measurements were carried out for different paramagnetic species: 1 mM aqueous solution of PADS at +21 °C, 1 mM aqueous solution of TEMPONE at +21 °C, 1 mM aqueous solution of TEMPOL in 80% glycerol at +21 °C and at +10 °C.

[a] $T_1$ of 0.9 mM water solution of PADS at +24 °C equal to 0.41 μs, reported in [35].

[b] $T_1$ of TEMPONE water solution at +20 °C equal to 0.64 μs ([35]).

tion times calculated from MQ-EPR experiments are compared with those obtained from saturation recovery and literature [35]. Data for the $T_1$ measured for TEMPOL solution in 80% glycerol at +10 and +20 °C to our knowledge, could not be found in the literature.

Three different systems have been studied: (a) $T_1 \cong T_2$ represented by PADS; (b) $T_1 \cong 3T_2$ as for TEMPONE in water ($\sigma \cong 0.\ 360$ MHz); (c) $T_1 > 10T_2$ represented by TEMPOL in glycerol ($\sigma \cong 2.13$ MHz). There is a good agreement between values obtained from SR EPR measurements and proposed procedure based on CW MQ EPR, even for inhomogeneous lines.

Both experimental methods are sensitive to true $T_1$. Application of a long, saturating pulse in saturation recovery EPR (for chosen samples, under conditions defined in Section 3.1) ensures that recovery of the signal is a single exponential trace. From the other side observation of multiquantum transitions requires that simultaneous transitions at $\omega_1$ and $\omega_2$ between electronic quantum levels are taking place. That coherence diminishes and disappears when the frequency difference is too big compared to $(T_1)^{-1}$. The shortest time measured by SR EPR is about 200 ns. In a multiquantum method one must shift the frequency difference up to about 1.3 MHz in order to notice the signal reduction. To measure relaxation times shorter than 200 ns that difference must grow. It does not complicate the experimental conditions provided that resonators with low $Q$ are used. It means that even shorter $T_1$'s can be measured. The proposed "multiquantum" method eliminates also the "phase problem" of the signal (e.g., very accurate setting of the signal phase is required in a method proposed by Livshitz et al. [19]).

## 4. Conclusions

Observation and interpretation of multiquantum transitions resulting from the interaction of two-level system with polychromatic irradiation is much easier with the help of developed model. Its important virtue is that signals resulting from different schemes of detection can be studied. Simulation of intermodulation sidebands gives a great help in choosing the best arrangement of the experimental observables and understanding the consequences of the "phase problems" of the detected signals. The proposed strategy of determining relaxation times from three quantum transition signals allows for omitting problems caused by uncontrolled change of signal phases. The information obtained from analysis yields the value of true $T_1$, whereas other CW methods (progressive saturation, observation of out-of-phase absorption signals) deliver $T_1$ effective. The ratio of the applied modulation (static magnetic field modulation or microwave field modulation) and $T_1$ of the "mixing" spin system is crucial for allowing the observation of the nonlinear response to perturbation. The "multiquantum" method fully exploits consequences of this fact. In other methods static magnetic field modulation is set arbitrarily, and for short longitudinal relaxation times may happen that $(T_1\omega_m) < 1$, what limits observation of nonlinear effects of higher order.

## Acknowledgment

This research was supported by the Science Research Committee Grant KBN Nos. P03B100 09 and 3P04A04323.

## References

[1] P.P. Borbat, A.J. Costa-Filho, K.A. Earle, J.K. Moscicki, J.H. Freed, Electron spin resonance in studies of membranes and proteins, Science 291 (2001) 266–269.
[2] W.L. Hubbell, C. Altenbach, Investigation of structure and dynamics in membrane proteins using site-directed spin labeling, Curr. Opin. Struct. Biol. 4 (1994) 566–573.
[3] J.S. Hyde, W. Froncisz, C. Motley, Pulsed ELDOR measurement of nitrogen $T_1$ in spin labels, Chem. Phys. Lett. 110 (1984) 621–625.
[4] B.S. Prabhananda, J.S. Hyde, Study of molecular motions in liquids by electron spin relaxation: halogenated *p*-semiquinone anions in alcohols, J. Chem. Phys. 85 (1986) 6705–6712.
[5] B.H. Robinson, D.A. Haas, C. Mailer, Molecular dynamics in liquids: spin lattice relaxation of nitroxide spin labels, Science 263 (1994) 490–493.
[6] L. Anreozzi, M. Giordano, D. Leporini, M. Martinelli, L. Pardi, Non-linear electron paramagnetic resonance spectroscopy: direct observation of slow dynamics effects at polymer glass transition, Phys. Lett. A 160 (1991) 309–314.
[7] I.J. van den Dries, P.A. de Jager, M.A. Hemminga, Sensitivity of saturation transfer electron spin resonance extended to extremely slow mobility in glassy materials, J. Magn. Reson. 131 (1998) 241–247.
[8] V.A. Livshitz, T. Pali, D. Marsh, Relaxation time determinations by progressive saturation EPR: effects of molecular motion and Zeeman modulation for spin labels, J. Magn. Reson. 133 (1998) 79–91.

[9] J.S. Hyde, W.K. Subczynski, in: L.J. Berliner, J. Reuben (Eds.), Biological Magnetic Resonance. Vol. 8. Spin Labeling: Theory and Applications, Plenum Press, New York, 1989, pp. 399–425.
[10] C. Altenbach, W. Froncisz, J.S. Hyde, W.L. Hubbel, Conformation of spin-labeled melittin at membrane surfaces investigated by pulse saturation recovery and continuous wave power saturation electron paramagnetic resonance, Biophys. J. 56 (1989) 1183–1191.
[11] S.S. Eaton, G.R. Eaton, in: L.J. Berliner, G.R. Eaton, S.S. Eaton (Eds.), Biological Magnetic Resonance: Distance Measurements in Biological Systems by EPR, Kluwer Academic Publishers, Dordrecht, 2002, pp. 2–21.
[12] J.S. Hyde, in: L. Kevan, R.N. Schwartz (Eds.), Time Domain Electron Spin Resonance, Wiley, New York, 1979, pp. 1–70.
[13] D. Haas, C. Mailer, B.H. Robinson, Using nitroxide spin labels. How to obtain T1e from continuous wave electron paramagnetic resonance spectra at all rotational rates, Biophys. J. 64 (1993) 594–604.
[14] F. Cianflone, F. Francia, D. Leporini, Measurement of the longitudinal relaxation time by continuous-wave, nonlinear electron spin resonance spectroscopies, J. Magn. Res. 131 (1998) 86–91.
[15] H.S. Mchaourab, S. Pfeninger, W.E. Antholine, J.S. Hyde, P.M. Kroneck, Multiquantum EPR of the mixed valence copper site in nitrous oxide reductase, Biophys. J. 64 (1993) 1576–1579.
[16] D.A. Haas, T. Sugano, C. Mailer, B.H. Robinson, Motion in nitroxide spin labels: direct measurement of rotational correlation times by pulsed electron double resonance, J. Phys. Chem. 97 (1993) 2914–2921.
[17] J.R. Harbridge, S.S. Eaton, G.R. Eaton, Electron spin-lattice relaxation in radicals containing two methyl groups, generated by *g*-irradiation of polycrystalline solids, J. Magn. Reson. 159 (2002) 195–206.
[18] J.R. Harbridge, S.S. Eaton, G.R. Eaton, Electron spin-lattice relaxation processes of radicals in irradiated crystalline organic compounds, J. Phys. Chem. A 107 (2003) 598–610.
[19] V.A. Livshits, T. Pali, D. Marsh, Spin relaxation measurements using first-harmonic out-of-phase absorption EPR signals, J. Magn. Reson. 134 (1998) 113–123.
[20] P. Bucci, M. Martinelli, S. Santucci, Response to double irradiation of a nuclear spin system: general treatment and new multiple quantum transitions, J. Chem. Phys. 53 (1970) 4524–4539.
[21] J.F. Freed, Multiple Electron Resonance Spectroscopy, Plenum Press, New York, 1979 p. 73.
[22] J.D. Baldeschwieler, Density matrix description of nuclear magnetic double resonance, J. Chem. Phys. 40 (1964) 459–472.
[23] D. Leporini, Relationship between a nonlinear response and relaxation induced by colored noise, Phys. Rev. A 49 (1994) 992.
[24] L. Andreozzi, C. Donati, M. Giordano, D. Leporini, Longitudinal relaxation induced by colored noise, Phys. Rev. E 49 (1994) 3488–3502.
[25] P.B. Sczaniecki, J.S. Hyde, W. Froncisz, Continuous wave multiquantum electron paramagnetic resonance spectroscopy. II. Spin-system generated intermodulation sidebands, J. Chem. Phys. 94 (1991) 5907–5916.
[26] M. Giordano, D. Leporini, M. Martinelli, L. Pardi, S. Santucci, C. Umeton, Double-modulation electron-spin-resonance spectroscopy: experimental observations and theoretical comprehensive interpretation, Phys. Rev. A 38 (1988) 1931–1936.
[27] M. Jeleń, W. Froncisz, Multiquantum electron paramagnetic resonance transitions excited in a two-level system by tetrachromatic microwave irradiation, J. Chem. Phys. 109 (1998) 9272–9279.
[28] H.S. Mchaourab, J.S. Hyde, Continuous wave multiquantum electron paramagnetic resonance spectroscopy. III. Theory of intermodulation sidebands, J. Chem. Phys. 98 (1993) 1768–1796.
[29] H.S. Mchaourab, J.S. Hyde, Dependence of the multiple-quantum EPR signal on the spin-lattice relaation time. Effect of oxygen in spin-labeled membranes, J. Magn. Reson. Ser. B 101 (1993) 178–184.
[30] M. Giordano, D. Leporini, M. Martinelli, L. Pardi, Nonlinear electron spin resonance techniques for the study of inhomogeneously broadened spectra, J. Chem. Phys. 88 (1988) 607–619.
[31] M. Jeleń, W. Froncisz, The description of the multiquantum effects in electron paramagnetic resonance spectroscopy using the Bloch equation, J. Chem. Phys. 108 (1998) 4563–4571.
[32] C.W. Gear, Numerical Initial Value Problems in Ordinary Differential Equations, Prentice-Hall, New Jersey, 1971.
[33] W. Froncisz, J.S. Hyde, The loop-gap resonator: a new microwave lumped circuit ESR sample structure, J. Magn. Reson. 47 (1982) 515–521.
[34] Ilnicki, J. Kozioł, T. Oleś, J. Kostrzewa, W. Galiński, R.J. Gurbiel, W. Froncisz, Saturation recovery EPR spectrometer, Mol. Phys. Rep. 5 (1994) 203–207.
[35] I. Bertini, G. Martini, C. Luchinat, Relaxation data tabulation, in: C.P. PooleJr., H.A. Farach (Eds.), Handbook of Electron Spin Resonance, American Institute of Physics, New York, 1994.